Mechanism of Ca-ATPase Inhibition by Melittin in Skeletal Sarcoplasmic Reticulum†

John C. Voss, James E. Mahaney, and David D. Thomas*

Department of Biochemistry, University of Minnesota Medical School, Minneapolis, Minnesota 55455

Received June 20, 1994; Revised Manuscript Received October 12, 1994®

ABSTRACT: We have previously shown that the basic, amphipathic peptide melittin inhibits the Ca-ATPase of the sarcoplasmic reticulum membrane by inducing large-scale aggregation of the enzyme via electrostatic cross-linking. To better understand the physical mechanism by which melittin-induced Ca-ATPase aggregation inhibits the enzyme, we have performed time-resolved phosphorescence anisotropy (TPA) and steady-state fluorescence experiments in combination with enzyme kinetic assays, utilizing (1) native and charge-modified melittin in order to characterize the peptide charge dependence of the melittin−SR interaction, and (2) various calcium levels in order to define the effect of melittin on the enzyme's E1 and E2 conformational equilibrium. TPA results showed that decreasing melittin's positive charge dramatically decreases the ability of the peptide to aggregate the enzyme, which correlates with a reduced potency of the modified peptide to inhibit enzymatic activity. Steady-state fluorescence of fluorescein isothiocyanate-labeled Ca-ATPase showed that melittin reduces Ca-ATPase affinity for calcium by shifting the enzyme's E1−E2 conformational equilibrium toward E2, but increasing calcium progressively reverses this shift. Kinetic experiments showed that melittin does not prevent ATP-dependent enzyme phosphorylation, but it completely inhibits P_i-dependent EP formation and substantially slows P_i release during steady-state cycling. We conclude that melittin-induced aggregation of the Ca-ATPase depends on the electrostatic interaction of the peptide with cytoplasmic Ca^{2+}-dependent sites on the enzyme, and that enforced Ca-ATPase protein−protein interactions inhibit the conformational transitions that facilitate phosphoenzyme hydrolysis.

The Ca-ATPase in fast-twitch skeletal sarcoplasmic reticulum (SR)[1] is a transmembrane protein of approximately 110 kD, which couples the transport of 2 mol of Ca^{2+} across the SR membrane per mole of ATP hydrolyzed (Inesi, 1985). A thoroughly tested and widely accepted model for the Ca-ATPase enzymatic cycle is shown in Scheme 1. In this model, the enzyme cycles between two fundamental conformations, E1 and E2, which couple ATP hydrolysis to calcium transport via differences in their affinities and vectorial specificities for ATP and Ca^{2+}. In the absence of substrates and/or ligands, the enzyme is in equilibrium between E1 and E2 (step 8), but micromolar calcium shifts this conformational equilibrium [$K_8 \approx 1 \times 10^{12}$ M^{-2} (Alonso & Hecht, 1990)] strongly toward E1, forming Ca_2•E1 (Inesi, 1985; Froud & Lee, 1986; Wakabayashi et al., 1990). ATP binds rapidly and with high affinity to Ca_2•E1 [step 1, (DuPont, 1980)], and a conformational change [Ca_2•E1•ATP to Ca_2•E1′•ATP (step 2)] activates the enzyme (Coan & Inesi; 1977; Petithory & Jencks, 1986; Obara et al., 1988; Lewis & Thomas, 1992) for ATP-dependent phosphoenzyme formation (Froehlich & Taylor, 1975; Petithory & Jencks, 1986). Calcium is translocated across the membrane (step 4) by a conformational change that isomerizes Ca_2•E1P to Ca_2•E2P (Froehlich & Heller, 1985). Following the release of calcium (step 5) from the enzyme into the SR lumen (Beeler & Keffer, 1984), E2P is hydrolyzed (step 6) to E2•P_i (de Meis, 1988; Wictome et al., 1992; Obara et al., 1988), after which P_i and Mg^{2+} are released [step 7 (de Meis, 1988)].

Scheme 1

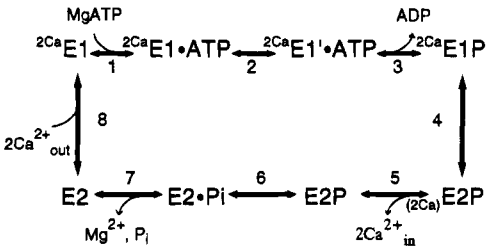

Extensive physical studies of skeletal SR have shown that the rotational dynamics of the Ca-ATPase have a substantial impact on Ca-ATPase activity (Thomas & Mahaney, 1993; Thomas & Karon, 1994), due to a requirement for dynamic changes in the oligomeric state of the enzyme during key steps the enzymatic cycle (Mahaney et al., 1994; Karon et al., 1994; Karon & Thomas, 1993; Bigelow et al., 1992; Martonosi et al., 1990; Squier & Thomas, 1988; Vanderkooi et al., 1977). Saturation transfer EPR studies of Ca-ATPase rotational dynamics (Thomas & Hidalgo, 1978; Bigelow et al., 1986) have shown that enzymatic activity correlates with the protein's rotational mobility, such that perturbations that decrease (increase) the Ca-ATPase mobility inhibit (enhance) enzymatic activity (Lewis & Thomas, 1986; Bigelow &

† This work was supported by a grant to D.D.T. from the National Institutes of Health (GM27906). J.E.M. was supported by a Grant-in-Aid from the American Heart Association, Minnesota Affiliate.

* To whom correspondence should be addressed.

® Abstract published in *Advance ACS Abstracts,* December 1, 1994.

[1] Abbreviations: SR, sarcoplasmic reticulum; MOPS, 3-(*N*-morpholino)propanesulfonic acid; ATP, adenosine triphosphate; EGTA, ethylene glycol bis(β-aminoethyl ether)-*N,N,N′,N′*-tetraacetic acid; TPA, transient phosphorescence anisotropy; ErITC, erythrosin-5-isothiocyanate.

0006-2960/95/0434-930$09.00/0

Thomas, 1987; Squier & Thomas, 1988; Squier et al., 1988a,b). Time-resolved phosphorescence anisotropy (TPA) measurements (Thomas, 1986; Birmachu & Thomas, 1990) of the Ca-ATPase oligomeric state show a strong correlation between conditions that inhibit Ca-ATPase activity and those that promote protein association, including some perturbations that have negligible effects on lipid fluidity (Birmachu & Thomas, 1990; Karon & Thomas, 1993; Karon et al., 1994).

We have previously investigated the effects of melittin, a basic amphipathic peptide from bee venom [reviewed by Dempsey (1990)], on Ca-ATPase dynamics and function using TPA (Voss et al., 1991) and EPR (Mahaney & Thomas, 1991; Mahaney et al., 1992), and these studies indicated that melittin binding to SR membranes inhibits Ca-ATPase activity by substantially increasing ATPase−ATPase association. Our results suggested a model for melittin-induced Ca-ATPase inactivation where the hydrophobic portion of the peptide partitions at the bilayer surface with its hydrophilic and basic portion free to interact with acidic residues on the cytoplasmic domain of the enzyme and thus electrostatically cross-link the ATPase into large aggregates.

Since the rotational dynamics and oligomeric state of the Ca-ATPase play a key role in modulating calcium uptake, it is important to understand the underlying mechanism relating these physical properties to the enzyme's kinetic behavior. Therefore, in the present study, we have investigated the physical and kinetic bases for the melittin-induced inhibition of Ca-ATPase activity. Since melittin is structurally analogous to the endogenous regulatory peptide, phospholamban, associated with the cardiac SR Ca-ATPase (Simmerman et al., 1986), and the autoregulatory domain of the plasma membrane Ca-ATPase (Vorherr et al., 1992), the results of this study provide insight into the mechanism of Ca-ATPase regulation by these physiological agents.

MATERIALS AND METHODS

Reagents and Solutions. Erythrosin-5-isothiocyanate (ErITC) was obtained from Molecular Probes, Inc. (Eugene, OR) and stored in DMF at −70 °C. ATP, bee-venom melittin (approx. 85% pure), catalase, glucose, glucose oxidase type IX, and poly(L-lysine) (MW 3200−3800) were obtained from Sigma Chemical Co. (St. Louis, MO). [γ-^{32}P]-ATP and [γ-^{32}P]PO_4^{3-} were obtained from New England Nuclear (Boston, MA). All other reagents were of the highest purity available. Assays and spectroscopic experiments were carried out at 25 °C in a buffer containing 60 mM KCl, 1 mM $MgCl_2$, 50 mM MOPS, pH 7.0, and either 0.1 mM $CaCl_2$ or 10 mM EGTA plus a sufficient amount of $CaCl_2$ to provide a given ionized calcium level. The free calcium concentrations of these buffers were determined using software developed by Fabiato (1988).

Preparations and Assays. Sarcoplasmic reticulum (SR) vesicles were prepared from the fast twitch skeletal muscle of New Zealand white rabbits (Fernandez et al., 1980). The vesicles were purified on a discontinuous sucrose gradient (Lewis & Thomas, 1992) to remove heavy SR vesicles (junctional SR containing calcium release proteins). Purified light and intermediate SR vesicles were harvested and then pelleted in 20 mM MOPS, pH 7.0. The pellets were resuspended in 0.3 M sucrose and 20 mM MOPS, pH 7.0 (henceforth denoted sucrose buffer), rapidly frozen, and stored in liquid nitrogen until use. All preparation was done at 4 °C. SR vesicles prepared in this fashion were typically 70% Ca-ATPase, determined by SDS−PAGE, and contained approximately 80 mol of phospholipid per mole of Ca-ATPase, determined by phosphorous assays (Chen et al., 1956). The SR vesicles prepared in this fashion are also predominantly right side out, as described by Campbell (1986).

SR Ca-ATPase activity was measured at 25 °C using an enzyme-linked, continuous ATPase assay, in the standard buffer with the addition of 20 μg/mL SR, 0.42 mM phosphoenolpyruvate, 0.15 mM NADH, 7.5 IU of pyruvate kinase, and 18 IU of lactate dehydrogenase. MgATP was added to start the assay, and the absorbance of NADH was monitored at 340 nm to determine the rate of ATP hydrolysis. All activity measurements were performed in the presence of 1 μg/mL of the ionophore A23187, which was added to SR prior to the start of the assays. Addition of the ionophore allows the Ca-ATPase activity to be measured in the absence of a Ca gradient, so that any vesicle leakiness produced by the addition of melittin will not affect the activity measured (Bigelow & Thomas, 1987). The activity measured in the presence of ionophore gives a maximal Ca-ATPase activity, since the enzyme does not have to work against a concentration gradient. SR protein concentrations were determined by the biuret assay (Gornall et al., 1949) using bovine serum albumin as a standard.

Melittin was purified by HPLC in the presence of 4 M urea, as described by Wille (1989), with the modifications outlined previously (Voss et al., 1991). Acetylation of the three lysine residues and the C-terminal amide on melittin was performed as described by Dufton et al. (1984). The fraction of melittin bound to SR was measured by melittin tryptophan fluorescence in the supernatant following centrifugation sedimentation of the SR vesicles, as described previously (Voss et al., 1991). Consistent with previous findings (Voss et al., 1991), nearly all native melittin added to SR binds to the vesicles. Acetylated melittin bound to SR with 12 ± 2% less potency than native melittin. To normalize for this difference, all melittin data report the amount of peptide bound per Ca-ATPase enzyme. Samples containing melittin were prepared by preincubating SR with the peptide in the experimental buffer for 20 min at room temperature, with intermittent gentle vortexing.

Ca-ATPase Labeling. For fluorescence and phosphorescence experiments, the Ca-ATPase in SR vesicles was labeled with FITC or ErITC, respectively, as described previously (Birmachu & Thomas, 1990). This procedure specifically labels Lys 515 on the Ca-ATPase, and results in enzyme inactivation, probably due to the labels' occupation of the nucleotide binding site (Birmachu & Thomas, 1990). However, extensive studies with skeletal SR labeled at this site with FITC show that the enzyme is otherwise unperturbed, has normal calcium binding, and goes through the normal calcium-pumping enzymatic cycle with less bulky substrates such as acetyl phosphate (Teruel & Inesi, 1988). Therefore, the conformational dynamics of FITC-SR are probably representative of the unlabeled protein, and, given the structural similarity between FITC and ErITC, the rotational dynamics of ErITC-SR are probably representative of the unlabeled protein. Labeled samples were kept on ice and used the same day for spectroscopic measurements.

Enzyme Phosphorylation Using P_i. Prior to phosphorylation, SR vesicles (0.5 mg/mL) were suspended in a buffer containing 10 mM $MgCl_2$, 2 mM EGTA, and 100 mM MOPS, pH 6.8. To initiate the phosphorylation reaction, an equal volume of 8 mM [^{32}P]Na_2HPO_4 in the same buffer was added to the SR vesicles and vortexed. The reaction was quenched after 5 min by the addition of 3% perchloric acid + 2 mM H_3PO_4 (final concentrations). The quenched vesicles were pelleted in a tabletop centrifuge and then washed three times with a solution of 5% trichloroacetic acid, 4 mM H_3PO_4, 6 mM polyphosphate, and 5 mM cold ATP. The final pellets were dissolved in 2 mL of 1 N NaOH overnight, and the [^{32}P]phosphoenzyme was assayed by counting the Cerenkov radiation.

Optical Spectroscopy. The experimental and analytical procedures for TPA of skeletal SR have been described in detail previously (Birmachu & Thomas, 1990; Birmachu et al., 1993). Oxygen was enzymatically removed from the TPA samples with 100 μg/mL glucose oxidase, 15 μg/mL catalase, and 5 mg/mL glucose, according to the method of Eads et al. (1984). Deoxygenation was carried out in a sealed cuvette (0.3 × 1.0 cm) containing 0.2−0.4 mg/mL SR protein for 10−15 min prior to phosphorescence data collection. The spectrometer used to obtain time-resolved phosphorescence anisotropy (TPA) decays was described previously (Ludescher & Thomas, 1988). The phosphorescence anisotropy decay r(t) is given by

$$r(t) = \frac{I_{vv} - GI_{vh}}{I_{vv} + 2GI_{vh}} \quad (1)$$

where I_{vv} and I_{vh} are the time-dependent decays of the phosphorescence intensities observed through polarizers oriented parallel and perpendicular, respectively, to the vertically polarized excitation pulse. G is an instrumental correction factor determined by measuring the anisotropy of free dye in solution under experimental conditions. TPA decays of ErITC-labeled Ca-ATPase were detected and signal-averaged for 20 loops, each consisting of 2000 acquisitions of I_{vv} and 2000 acquisitions of I_{vh}. The laser repetition rate was 100−200 Hz, so a typical measurement lasted about 10 min. Fluorescence spectra of FITC-labeled Ca-ATPase in SR were obtained with a SPEX Fluorolog II fluorometer using an excitation wavelength of 495 nm and an emission wavelength of 525 nm.

TPA Data Analysis. TPA decays were analyzed as reported previously (Birmachu & Thomas, 1990), using a nonlinear least-squares fit to a sum of exponentials plus a constant:

$$\frac{r(t)}{r(0)} = A(t) = \sum_{i-1}^{n} A_i e^{-t/\phi_i} + A_\infty \quad (2)$$

where ϕ_i are rotational correlation times, A_i are the normalized amplitudes (r_i/r_0), A_∞ is the normalized residual anisotropy (r_∞/r_0), and r_0 is the initial anisotropy [$r(0) = r_0 = \sum r_i + r_\infty$]. The goodness-of-fit for the anisotropy decays was evaluated by comparing χ^2 values for the multiexponential fits and by comparing plots of the residuals (the difference between the measured and the calculated values).

It has been shown previously (Birmachu & Thomas, 1990) that the TPA of ErITC-SR is dominated by the uniaxial rotation of the labeled Ca-ATPase about an axis normal to the bilayer. For this model, each different rotational diffusion coefficient should give rise to a biexponential decay component [Kinosita et al., 1984; reviewed by Thomas (1986)], but it has been shown that a single-exponential approximation is sufficient to describe the decay for each rotating species in ErITC-SR (Birmachu & Thomas, 1990). As long as the probe orientation relative to the protein is the same for all proteins, the mole fraction (f_i) of probes in the ith rotating species, having rotational correlation time ϕ_i, is given by

$$f_i = A_i/(1 - A_{\infty 0}), \quad f_I = (A_\infty - A_{\infty 0})/(1 - A_{\infty 0}) \quad (3)$$

where f_I is the fraction of probes (proteins) that are immobile on the time scale of the experiment (Birmachu et al., 1993). $A_{\infty 0}$ is the residual anisotropy of a reference sample for which $f_I = 0$ and describes the extent to which the probe's motion is restricted in angular range, due to the fixed angles θ_{ma}, and θ_{me} of the probe's absorption and emissions transition moments relative to the membrane normal:

$$A_{\infty 0} = \frac{P_2(\cos\theta_{ma})P_2(\cos\theta_{me})}{P_2(\cos\theta_{ae})} \quad (4)$$

where $P_2(x) = (3x^2 - 1)/2$, and θ_{ae} is the angle between the absorption and emission transition moments (Lipari & Szabo, 1980). $A_{\infty 0}$ has been shown to be 0.22 for ErITC-Ca-ATPase in skeletal SR (Birmachu & Thomas, 1990).

The rotational diffusion coefficient (D_m) for uniaxial rotation of a cylindrical membrane protein can be expressed as a function of the membrane lipid viscosity (η), the temperature (T), and the effective radius (a) of the portion of the protein in the bilayer (Saffman & Delbrück, 1975):

$$D_m = \frac{kT}{4\pi a^2 h\eta} \propto \frac{1}{\phi} \quad (5)$$

where h is the thickness of the hydrocarbon phase of the lipid bilayer. Thus, the rotational correlation time (inversely proportional to the diffusion coefficient) should be proportional to the lipid viscosity (inverse of fluidity) and to the intramembrane cross-sectional area (πa^2) of the rotating protein. This theory relating protein size and lipid fluidity to protein rotational mobility is supported by previous studies on the Ca-ATPase as measured by both ST-EPR (Squier et al., 1988a,b) and phosphorescence anisotropy (Birmachu & Thomas, 1990). Mahaney and Thomas (1991) have shown that melittin binding to SR membranes has only small effects on the bilayer fluidity (T/η), and these changes are much too small to account for melittin-induced changes in Ca-ATPase rotational mobility. Therefore, any melittin-dependent changes in the observed rotational correlation times must be due to changes in the effective radius (a in eq 5) of the rotating protein. The only plausible source of large changes in protein size in SR is protein association into different sized oligomers, with the rotational correlation time ϕ_i roughly proportional to the size of the oligomer (Birmachu & Thomas, 1990). Thus the distribution of oligomeric species is given by the fractions f_i (eq 3). The fraction of proteins in immobile species f_I, determined from the residual anisotropy A_∞, thus corresponds to protein aggregates so large that they undergo little or no rotational diffusion in the 1-ms time window of the TPA experiment. Since the correlation time of a Ca-ATPase monomer or dimer is on the order of 10−

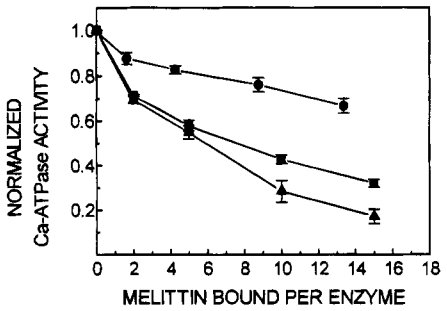

FIGURE 1: Effect of acetylated melittin (●), native melittin (■), and native melittin after preincubation of SR at 0.01 μM Ca^{2+} (▲), on Ca-ATPase activity at 25 °C. Enzyme-linked ATPase assays were measured in a buffer containing 10 μM Ca^{2+} as described under Materials and Methods. Errors represent the standard error of the mean from five separate experiments.

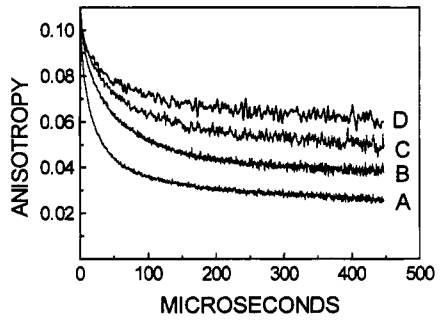

FIGURE 2: Time-resolved phosphorescence anisotropy decays of ErITC-labeled Ca-ATPase in SR vesicles at 25 °C. (A) Control SR without added melittin; (B) SR with 10 mol of acetylated melittin *bound* per mol of Ca-ATPase; (C) SR with 10 mol of native melittin bound per mol of Ca-ATPase enzyme; (D) SR preincubated with 10 mol of native melittin per mol of Ca-ATPase in the presence of 0.01 μM Ca^{2+} and then transferred into the standard experimental solution containing 10 μM Ca^{2+}.

20 μs, these immobile aggregates must contain more than 10 Ca-ATPase molecules (Birmachu & Thomas, 1990; Voss et al., 1991; Birmachu et al., 1993).

RESULTS

Melittin Inhibits Ca-ATPase Activity and Enzyme Rotational Mobility. Melittin binding to SR strongly inhibits Ca-ATPase activity, with 50% inhibition occurring at about 8 mol of melittin per mol of ATPase (Figure 1). Melittin binding to SR also substantially decreases the rotational mobility of the Ca-ATPase. The TPA decays obtained from ErITC-labeled Ca-ATPase in Figure 2 show that the anisotropy of the enzyme in the presence of 10 mol of melittin per mol of ATPase (trace C) is greater than in control SR membranes without added melittin (Trace A). We have previously demonstrated (Voss et al., 1991) that melittin affects the component amplitudes (A_i in eq 2) but not the component rates ($1/\phi_i$ in eq 2) of the anisotropy decay; that is, melittin decreases Ca-ATPase rotational mobility by aggregating smaller, more mobile enzyme units into larger, less mobile enzyme units, rather than slowing the rates at which each component rotates (Mahaney & Thomas, 1991).

In a previous study, we found that increasing the ionic strength of the incubation medium decreases melittin-induced inhibition of both Ca-ATPase inhibition and aggregation. Given that there is only a trace amount of acidic lipids in SR (Hidalgo, 1987) that could interact directly with melittin, and that the Ca-ATPase is the predominant protein species

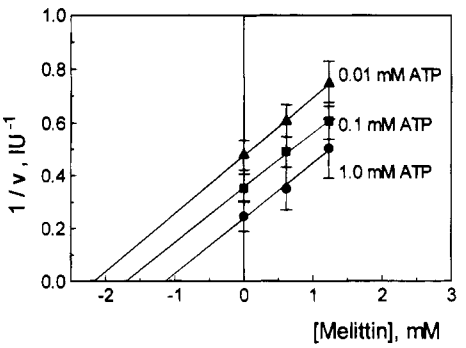

FIGURE 3: Dixon plots showing that melittin is an uncompetitive inhibitor of the Ca-ATPase. The concentration of bound melittin is given on the abscissa. Enzyme-linked ATPase assays were performed at 25 °C in a buffer containing 10 μM Ca^{2+} as described under Materials and Methods. The lines are the best fit by least-squares analysis to the data at each ATP concentration, and the apparent K_I, 1.8 ± 0.5 μM, was determined as described under Results. Errors represent the standard deviation of three separate measurements.

in our SR preparation (70% total protein), this result suggested that electrostatic interaction between melittin's basic charges and known acidic residues on the Ca-ATPase stalk domain (Asturias et al., 1994) plays a primary role in melittin-induced enzyme inhibition (Voss et al., 1991). In the present study, we tested the electrostatic interaction proposal directly by studying the efficacy of a charge-modified melittin to inhibit and aggregate the enzyme. For this experiment, we reduced the basic charge on melittin from +5 to +2 by acetylating the peptide (Dufton et al., 1984). Acetylated melittin (a) inhibits ATPase activity with only half the potency of native melittin (Figure 1) and (b), at 10 moles bound per mole ATPase, increases the anisotropy of the enzyme (Figure 2, trace B) to only half the extent as native melittin (Figure 2, trace C) relative to control enzyme without added melittin (Figure 2, trace A), consistent with the proposal that melittin's basic residues play an important role in its ability to inhibit and aggregate the Ca-ATPase. In fact, decreasing the positive charge on melittin protects Ca-ATPase mobility (Figure 2) and activity (Figure 1) to the same extent (50%), strengthening our previous conclusion that melittin binding to SR inhibits the Ca-ATPase by converting optimally active Ca-ATPase monomers and small oligomers into inactive large-scale aggregates (Voss et al., 1991; Mahaney & Thomas, 1991). Since melittin-induced aggregation of the Ca-ATPase correlates with the loss of ATPase activity, we next investigated the mechanistic consequences of melittin-induced Ca-ATPase aggregation.

Melittin Is an Uncompetitive Inhibitor of the ATPase. In order to characterize the mechanism of melittin's inhibition of the Ca-ATPase, we measured the inhibitory effects of melittin at several ATP concentrations. The Dixon plot of these data (Figure 3) indicates that melittin is an uncompetitive inhibitor of the Ca-ATPase (Segel, 1976), with an apparent K_i of 1.8 ± 0.5 μM. As an uncompetitive inhibitor of the enzyme, melittin should inhibit V_{max} *and* decrease K_m. To test this, we measured the inhibitory effects of the peptide over a large ATP concentration range (0.001, 0.005, 0.01, 0.05, 0.1, 0.5, and 1.0 mM). Melittin reduced ATPase activity over the entire ATP concentration range and analysis of the double-reciprocal plot of the V vs [ATP] data (Segel, 1976) confirmed that the peptide (at 10 mol of melittin per

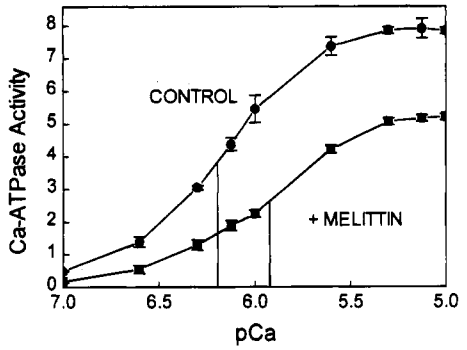

FIGURE 4: Effect of melittin on the Ca^{2+}-dependence of Ca-ATPase activity. SR vesicles were preincubated either without melittin (●) or with 10 mol of melittin per mol of ATPase (■) and assayed for activity at the indicated ionized Ca^{2+} concentration using the enzyme-linked assay described under Materials and Methods. The dashed lines indicate the Ca^{2+} concentration where Ca-ATPase activity was 50% the maximal level. Errors represent the difference between two separate measurements.

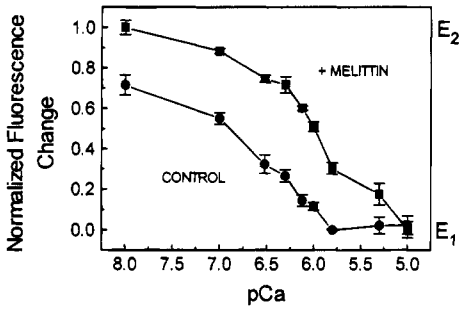

FIGURE 5: Effect of calcium and melittin on the Ca-ATPase E_1-E_2 conformational equilibrium, as measured by the relative fluorescence intensity of FITC bound to Lys 515 on the enzyme. FITC-SR vesicles were preincubated either without melittin (●) or with 10 mol of melittin per mol of ATPase (■) and analyzed at the indicated ionized Ca^{2+} concentration. Errors represent the standard deviation of three separate measurements.

mol of ATPase) inhibited V_{max} by 45% *and* decreased K_m by 36%.

Melittin Reduces the Ca-ATPase's Calcium Affinity. We measured melittin's effects on the calcium concentration dependence of the Ca-ATPase activity (Inesi, 1985). Figure 4 shows that at each Ca^{2+} concentration studied, melittin (at a level of 10 mol of melittin per mol of Ca-ATPase) reduces ATPase activity relative to the control enzyme in the absence of melittin. Comparison of the K_{Ca} (dashed lines, Figure 4) in the absence and presence of melittin shows that the peptide shifts the calcium concentration dependence of ATPase activity by nearly 0.25 pCa units, consistent with the interpretation that melittin reduces the enzyme's affinity for calcium.

Melittin Shifts the Ca-ATPase E1−E2 Conformational Equilibrium. The steady-state fluorescence emission of fluorescein isothiocyanate (FITC) bound to Lys 515 of the Ca-ATPase has been shown to be a sensitive measure of the E1−E2 conformational equilibrium (Froud & Lee, 1986). In response to increasing Ca^{2+} concentration, the relative FITC fluorescence of the control enzyme without added melittin decreased (Figure 5) as the conformational equilibrium of the enzyme shifted toward the E1 state. The addition of melittin (at a level of 10 mol of per mol of ATPase) to FITC-SR incubated at various Ca^{2+} concentrations increased the fraction of enzyme in the E2 state at each Ca^{2+} level.

Table 1: Effect of Melittin (MLT) on the Fluorescence Intensity of FITC-LSR at 25 °C[a]

FITC-LSR sample (ionized $[Ca^{2+}]$)	Intensity ($\times 10^{-7}$)	ΔF (corr)
initial 100 μM Ca (100 mM)	5.02 ± 0.16	
add 0.5 mM EGTA (100 nM)	5.27 ± 0.09	8%
initial 100 mM Ca (100 μM)	4.98 ± 0.21	
add 10:1 MLT (100 μM)	4.85 ± 0.13	0%
after 5 min incubation	4.85 ± 0.14	0%
after 20 min incubation	4.85 ± 0.10	0%
add 0.5 mM EGTA (100 nM)	4.85 ± 0.15	0%
after 5 min incubation	4.98 ± 0.09	3%
after 20 min incubation	5.32 ± 0.01	10%
initial 1 mM EGTA (0)	5.51 ± 0.01	
add 1 mM Ca (100 μM)	5.04 ± 0.01	−6%
initial 1 mM EGTA (0)	5.31 ± 0.08	
add 10:1 MLT (0)	5.20 ± 0.05	1%
after 5 min incubation	5.34 ± 0.08	4%
after 20 min incubation	5.80 ± 0.15	12%
add 1 mM Ca (100 μM)	5.70 ± 0.18	11%
after 5 min incubation	5.70 ± 0.20	11%
after 20 min incubation	5.70 ± 0.25	11%

[a]Intensity of FITC-LSR fluorescence measured as described under Materials and Methods. The samples were prepared in a buffer containing either 100 μM Ca^{2+} or 1 mM EGTA (designated "initial"), and subsequent additions of either melittin (denoted MLT), EGTA, or Ca^{2+} were made as indicated. The ionized calcium concentration (given in parentheses after each sample) was calculated as described previously (Voss et al., 1994). The total intensity represents the average of 2−3 experiments, and the errors listed are either the standard deviations (n = 3) or the difference from the mean (n = 2). ΔF (corr) is percent change ($F - F_0/F_0$) from control (either 100 μM Ca or 1 mM EGTA) corrected for the effects of sample dilution (ΔF_{dil} = 3%), which was calculated by adding an equal volume of water to the sample under experimental conditions.

However, above 1 μM Ca^{2+}, melittin became less effective at shifting the conformation toward E2, and by 10 μM Ca^{2+} the peptide was unable to shift the enzyme conformation toward E2 at all. The results of Figure 5 provide a physical basis for the observed shift in the enzyme's calcium affinity: more calcium is required to overcome the melittin-induced shift of the enzyme's E1−E2 equilibrium toward E2. Figure 5 also suggests that melittin's interaction with the Ca-ATPase may be dependent on ATPase conformation.

Ca-ATPase Conformation Affects the Potency of Melittin Inhibition. Since melittin shifted the enzyme's E1−E2 conformational equilibrium toward E2 more strongly at low Ca^{2+} concentration than at high Ca^{2+} concentration, which shifts the control enzyme toward E1, we tested whether melittin preferentially interacts with the enzyme in the E2 form relative to the E1 (Table 1). We found that addition of 0.5 mM EGTA to FITC-SR in the presence of 100 μM Ca^{2+} (change in Ca^{2+} concentration from 100 μM to 100 nM) increased FITC fluorescence by 8%, consistent with a shift in the E1−E2 conformational equilibrium toward E2 (Karon et al., 1994). This change was instantaneous and stable over 60 min of observation. Addition of 1.1 mM $CaCl_2$ to FITC-SR in the presence of 1 mM EGTA (change in Ca^{2+} concentration from 0 to 100 μM) decreased FITC fluorescence by 6%, consistent with a shift in the E1−E2 conformational equilibrium toward E1 (Karon et al., 1994). As before, the change was instantaneous and stable over 60 min of observation. The addition of 10 mol of melittin per mol of ATPase did not affect the intensity of FITC-SR in the presence of 100 μM Ca^{2+} (>99% E1; Alonso & Hecht,

1990), even after 20 min. However, in response to the addition of EGTA after melittin, the fluorescence intensity increased in a time-dependent manner to 10%, a level which is greater than that induced by the addition of EGTA alone (Table 1). The addition of 10 mol of melittin per mol of Ca-ATPase to FITC-SR in the presence of 1 mM EGTA (which favors the E2 conformation) induced an initial increase (1%) in the fluorescence intensity, and the intensity continued to increase in a time-dependent manner, reaching 12% at 20 min after the addition of melittin. Subsequent addition of 1.1 mM $CaCl_2$ had no significant effect on the fluorescence intensity. All of the values listed in Table 1 are shown corrected for the effects of sample dilution caused by successive additions of reagents (see Table 1). These results demonstrate that melittin has no effect on the E1 conformation of the enzyme and does not block the E1 to E2 transition; rather, melittin preferentially interacts with the E2 form of the enzyme, stabilizing that form of the enzyme and preventing the E2 to E1 transition.

The functional and physical consequences of this preferential interaction between melittin and the enzyme's E2 conformation were also investigated. The experiments of Figure 1 and 2 were repeated (using native melittin only) except that the SR was preincubated with melittin in the presence of 0.01 μM Ca^{2+}, prior to transferring the sample into the measurement medium which contained 10 μM Ca^{2+}. Under these conditions (which favor E2, Figure 5), melittin both inhibited (Figure 1) and aggregated (Figure 2, trace D) the Ca-ATPase more potently than when the preincubation buffer contained 10 μM calcium (which strongly promotes the ^{2Ca}E1 form of the enzyme). These Ca^{2+}-dependent effects were only observed at higher melittin levels (e.g., more than 5 mol of melittin per mol of ATPase), where melittin-ATPase interactions are characterized by electrostatic forces (Voss et al., 1991). Thus, the enhanced interaction between the peptide and the enzyme's E2 conformation is due to enhanced electrostatic interaction between melittin and the ATPase, presumably at Ca-dependent sites coupled to the E1−E2 transition. Our finding that the enhanced melittin inhibition and aggregation following the 0.01 μM Ca^{2+} preincubation is maintained even after transferring the sample into the assay medium containing 10 μM Ca^{2+} suggests that the interactions between the Ca-ATPase and melittin formed in the absence of calcium are very stable and not rapidly reversed.

Effect of Melittin on Enzyme Phosphorylation by P_i. In a final set of experiments, we tested whether the enzyme preincubated with melittin at low calcium ([Ca^{2+}] < 0.01 μM) could undergo phosphorylation by P_i, and we studied the effect of melittin on enzyme phosphorylated by P_i prior to the addition of melittin. Table 2 shows that melittin decreases the enzyme's ability to undergo phosphorylation by P_i. The same levels of phosphoenzyme were observed when melittin was added *after* enzyme phosphorylation. This result suggests that by stabilizing the E2 conformation of the enzyme, melittin prevents the enzyme from undergoing the conformational change required to accept the phosphate molecule in the formation of E2P (Sagara et al., 1992a; Wictome et al., 1992), thus shifting the E2 + P_i = E2P equilibrium strongly toward E2 + P_i.

Table 2: Effect of Melittin on Ca-ATPase Phosphorylation by P_i[a]

melittin (mol/mol of Ca-ATPase)	EP (nmol/mg of SR)
0	1.25 ± 0.2
2	0.77 ± 0.04
5	0.52 ± 0.06
7	0.23 ± 0.02
10	0.21 ± 0.04

[a]Enzyme phosphorylation was carried out as described under Materials and Methods. SR samples were preincubated with melittin for 20 min prior to phosphorylation. The same results were obtained when melittin was added to SR after phosphorylation (not shown). Errors represent the standard deviations of four separate measurements.

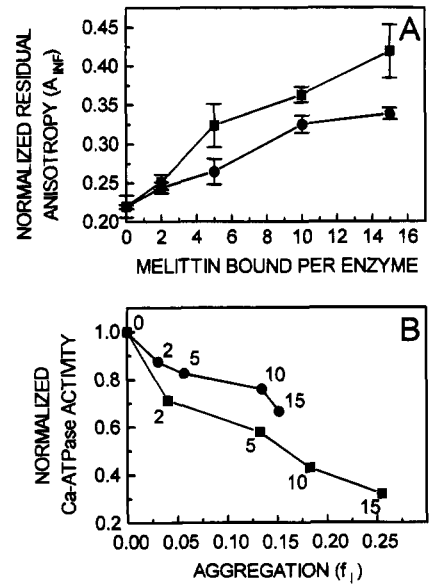

FIGURE 6: (A) Effect of acetyled melittin (●) and native melittin (■) on the normalized residual anisotropy (A_∞) from a three-exponential fit of the ErITC-labeled Ca-ATPase TPA decay (see Materials and Methods). (B) Correlation of the fraction Ca-ATPase in large-scale aggregates [$f_I = (A_\infty - 0.22)/(1 - 0.22)$; see Discussion] with enzyme activity in the presence of various levels of acetylated melittin (●) and native melittin (■). In panel B, numbers by the data points indicate the amount of melittin added (mol) per mol of Ca-ATPase. Errors represent the standard deviations of three separate measurements.

DISCUSSION

Molecular Interpretation of Results. Melittin binding to the SR membrane inhibits Ca-ATPase activity (Figure 1). The peptide also restricts Ca-ATPase mobility (Figure 2), as indicated by melittin-induced increases in the normalized residual anisotropy (A_∞, Figure 6A). Figure 6B shows the relationship between the melittin's inhibition of Ca-ATPase activity (from Figure 1) and melittin's increase in the fraction of Ca-ATPase that exists as large, immobile aggregates (f_I), calculated from the normalized residual anisotropy (A_∞, Figure 6A) using eq 3, with $A_\infty = 0.22$ (Birmachu & Thomas, 1990). There is a strong correlation between Ca-ATPase aggregation and inactivation (Figure 6), consistent with the proposal by Voss et al. (1991) that melittin induces large-scale Ca-ATPase aggregation, forcing the enzyme into a kinetically unfavorable state.

The Role of Electrostatic Interactions between Melittin and the Ca-ATPase. We have previously shown that melittin's effects on Ca-ATPase activity and mobility are decreased

by high ionic strength (Voss et al., 1991; Mahaney & Thomas, 1991), suggesting that electrostatic interaction between the peptide's basic residues and acidic residues on the enzyme play a role in the observed inhibition. Therefore, we investigated the role of melittin's basic charge by acetylating the peptide's lysine residues, which decreases the net charge of the peptide from +5 to +2. The ability of acetylated melittin to both inhibit (Figure 1) and immobilize the enzyme (Figure 2) is markedly reduced by this charge decrease. The relationship between activity and aggregation is similar for normal and acetylated melittin (Figure 6B), suggesting that the decreased ability of acetyl melittin to inhibit the Ca-ATPase is reflected by its decreased ability to immobilize the enzyme in large aggregates. We conclude that melittin's basic (i.e., lysine) residues play a substantial role in the peptide's ability to aggregate and inhibit the Ca-ATPase. Werkmeister et al. (1993) have recently shown that melittin's arginine residues are also important to the cytolytic activity of the peptide, suggesting that future studies should be directed at understanding the role of melittin's two arginine residues in aggregating and inhibiting the ATPase.

Since the regulatory effects by structurally analogous peptides on other Ca^{2+}-transporting ATPases (Toyofuku et al., 1993; Vorherr et al., 1992) are exerted significantly only in the submicromolar Ca^{2+} range, we investigated the Ca^{2+} dependence of melittin's effects on the Ca-ATPase. When melittin is preincubated with the SR vesicles at very low (0.01 μM) Ca^{2+} prior to data collection, melittin-induced inhibition (Figure 1) and large-scale Ca-ATPase aggregation (Figure 2) are enhanced, but only at higher melittin levels (>5 mol of melittin per mol of ATPase). Since this is the range where melittin−ATPase interactions are dominated by electrostatic forces (Voss et al., 1991; Mahaney & Thomas, 1991), and Ca^{2+} modulates this interaction, melittin's basic residues may be interacting with the ATPase at negatively charged, cation binding residues in the Ca-ATPase stalk domain that have recently been characterized by Asturias et al. (1994). The extent to which low Ca^{2+} enhances melittin's effects on activity and mobility is similar, thus strengthening the correlation between Ca-ATPase association state and functional state, and the role that electrostatics play in the melittin-ATPase interaction.

Conformational Consequences of Melittin-Induced Enzyme Aggregation. It has been shown previously in this laboratory that inhibitors that aggregate the Ca-ATPase also shift its conformational equilibrium toward the E2 forms (i.e., E2, E2P, and/or $_{(2Ca)}$E2P in Scheme 1) (Karon et al., 1994). We found that melittin also shifts the E1/E2 equilibrium toward E2 (Figure 5), and the shift is greater at low Ca^{2+} concentration (< 1 μM) than at high Ca^{2+} concentration. Figure 7 shows that melittin-induced enzyme aggregation is also more extensive at low Ca^{2+} concentration than at high, strengthening the correlation between aggregation and stabilization of the E2 conformation. Modulating Ca^{2+} concentration has no effect on f_l in control SR without added melittin (Figure 7), suggesting that the enzyme does not self-aggregate in response to a shift in the E1−E2 conformational equilibrium toward E2. Rather, it appears that melittin-induced aggregation stabilizes E2, thus decreasing Ca^{2+} affinity and shifting the Ca^{2+} dependence of ATPase activity (Figure 4). We cannot, however, rule out any direct interaction between the peptide and the bound FITC probe, because we do not know the exact site of melittin binding to the Ca-ATPase. Future studies directed toward localizing the interaction site(s) of the peptide on the enzyme (cf. Cuppoletti, 1990; Cuppoletti et al., 1990) should provide insight into this possibility.

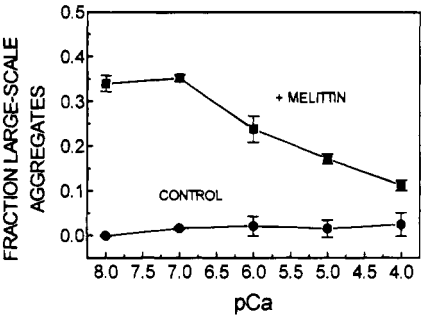

FIGURE 7: Ca^{2+} dependence of melittin-induced immobilization of the Ca-ATPase in SR vesicles in the absence (●) or presence (■) of 10 mol of melittin per mol of Ca-ATPase. The fraction of large-scale enzyme aggregates (f_l) at each ionized Ca^{2+} level was calculated as described under Materials and Methods. Errors represent the standard deviations of three separate measurements.

We also investigated whether the melittin-stabilized E2 form of the enzyme is able to undergo phosphorylation by P_i (Table 2), since E2 is the most P_i-reactive state. The phosphorylation conditions ([Ca^{2+}] < 10 nM) were selected to maximize E2P formation (Chaloub et al., 1979), which also maximizes melittin-induced enzyme aggregation (Figure 6). Melittin almost completely eliminates EP formation when the peptide is added to SR prior to phosphorylation, and the peptide reduces EP levels almost completely when added to SR under steady-state phosphorylation conditions. We conclude that the melittin-induced aggregation that stabilizes E2 also blocks subsequent conformational transition(s) necessary for the formation and stabilization of E2P (Wictome et al., 1992).

This effect of melittin on EP formation from P_i is opposite to that observed for the effects of the Ca-ATPase specific inhibitor thapsigargin (TG). TG, like melittin, stabilizes the enzyme in the E2 form (Sagara et al., 1992a). However, Sagara et al. (1992b) have demonstrated that TG decreases EP levels by only 50%, and that the TG−E2-stabilized enzyme can be phosphorylated by P_i (up to 50% of the control level) even in the presence of 35 μM Ca^{2+}. A key difference between TG and melittin is that TG pushes the Ca-ATPase from E1 to E2 prior to aggregating the enzyme (Mersol et al., 1995), whereas large-scale enzyme aggregation probably precedes melittin-induced E2 stabilization and Ca-ATPase inhibition. If the aggregated enzyme cannot in fact undergo the conformational change required for phosphorylation by P_i, this difference explains why TG-Ca-ATPase is phosphorylated by P_i whereas the melittin-Ca-ATPase is not. Support for this interpretation is provided by Karon et al. (1994) who have shown that cyclopiazonic acid (CPA), which also promotes enzyme aggregation, prevents enzyme phosphorylation by P_i. This highlights the need for caution when describing the enzyme in two principle states, as several substates exist with different chemical and physical properties. Future experiments designed to test the effects of melittin on each of the Ca-ATPase partial reactions should help define which transition(s) between Ca-ATPase E1 and E2 conformational substrates are inhibited by the peptide, with concomitant inhibition of the whole cycle.

Mechanistic Consequences of Melittin-Induced Enzyme Aggregation. Saturating Ca^{2+} (10 μM) decreases melittin's

ability to aggregate the Ca-ATPase and prevents melittin from shifting the E1−E2 equilibrium toward E2 (Figure 5 and Table 1). However, when the enzyme is in the E2 form, melittin-induced aggregation is maximized, and melittin strongly stabilizes the enzyme against Ca^{2+}-induced shifts to the E1 form (Table 1). Therefore, under the conditions of the steady-state ATPase assay (0.01 mM Ca^{2+}) shown in Figure 1, melittin inhibition of enzyme activity can be interpreted in terms of the stabilization of E2, via enzyme aggregation, as the enzyme cycles. Figure 3 shows that melittin is an uncompetitive inhibitor of the Ca-ATPase, indicating the peptide decreases the enzyme's V_{max} (defined as $k_{cat}[E]_{tot}$). Since Voss et al. (1991) have demonstrated that melittin binding to SR membranes is quantitative and essentially irreversible, we conclude that the peptide inhibits Ca-ATPase activity by forcing the enzyme (via aggregation) into a stable enzyme−melittin complex (i.e., E2−melittin), thus reducing $[E]_{tot}$, with apparent loss of activity.

Kinetic and spectroscopic evidence supports the proposal that the Ca-ATPase enzymatic cycle (Scheme 1) involves a dimeric enzyme complex with coupled subunits, such that the E1 (or E1P) to E2 (or E2P) transition in one subunit is coupled to the E2 (or E2P) to E1 (or E1P) transition in the other subunit (Froehlich & Heller, 1985; Mahaney et al., 1994). Karon et al. (1994) have shown that either over-stabilizing Ca-ATPase oligomers with cyclopiazonic acid or excessively depleting enzyme oligomers with halothane (Karon & Thomas, 1993) inhibits the enzyme, suggesting that oligomeric interactions are necessary to optimize conformational changes in the coupled subunits. Voss et al. (1991) have previously demonstrated that melittin promotes large-scale aggregation of the Ca-ATPase by converting optimally active and mobile Ca-ATPase monomers and small oligomers into less active, intermediate sized oligomers (less than 10 ATPase units) that display substantially restricted mobility. These intermediate oligomers are, in turn, converted into inactive and immobile large aggregates (>10 ATPase units). At the level of 10 mol of melittin per mol of ATPase, where ATPase activity is inhibited by 60%, we find that 25% of the enzyme exists as large-scale aggregates (Figure 6B) and 35% of the enzyme exists as intermediate sized oligomers (data not shown; cf. Voss et al., 1991). The role that the intermediate aggregates play in the mechanism of melittin-induced enzyme inhibition is not well understood, yet the sum of the mole fractions of these oligomers and that of the immobile aggregates matches the level of ATPase inactivation we observed. This result suggests that any enforced aggregation beyond dimers and tetramers is detrimental to Ca-ATPase activity, due to the restriction of either conformational changes within subunits or oligomeric changes in the Ca-ATPase.

Relationship to Other Systems. The interaction of melittin with other proteins suggests that proteins with metal ion binding sites may be targets for amphipathic peptide regulation. Melittin inhibits the Na^+,K^+-ATPase and the H^+,K^+-ATPase, but these enzymes can be protected against melittin inhibition by increasing the levels of the transported ion (Cuppoletti et al., 1992; Cuppoletti & Abbot, 1990). The sensitivity of the melittin−enzyme interaction to the level of Ca^{2+} in the 0.01−10 μM range suggests involvement of residues on the Ca-ATPase which have relatively high affinity for Ca^{2+}. Melittin interacts strongly with several other acidic, Ca^{2+} -binding proteins including protein kinase C (Gravitt et al., 1993), phosphorylase kinase (Paudel et al., 1993), calsequestrin (He et al., 1993), calmodulin (Malencik & Anderson, 1985), and acyl carrier protein (Ernst-Fonberg, 1990). Lanthanides bind with high affinity to acidic residues on the stalk domain of the Ca-ATPase (Sprowl & Thomas et al., 1989; Asturias et al., 1994; Henao et al., 1992; Asturias & Blasie, 1991; Itoh & Kawakita, 1984). Although lanthanide binding to these sites displaces Ca^{2+}, these residues are separate from the high-affinity Ca^{2+} transport sites which are located in the transmembrane domain (Clarke et al., 1989). Asturias et al. (1994) have recently provided physical evidence suggesting that these residues play a role in directing Ca^{2+} toward its high-affinity transport sites on the enzyme during ATPase conformational changes. The results of the present study show that, by binding to these sites and promoting large-scale enzyme aggregation, melittin disrupts the affinity for Ca^{2+} and key conformational changes related to enzyme turnover.

The interaction of melittin with the Ca-ATPase in SR provides insight into the functional consequences of Ca-ATPase self-association. On a more general level, this interaction is also an excellent model system for the study of the regulation of P-type ion pumps by endogenous amphipathic peptides. The SR Ca-ATPase in cardiac SR (and to a lesser extent in smooth and slow-twitch muscle SR) and the plasma membrane Ca-ATPase are regulated by analogous basic, amphipathic peptide structures. In cardiac SR, Ca-ATPase regulation by phospholamban (PLB) shares several characteristics with the melittin−SR system. The interaction of the hydrophilic portion of PLB (residues 1−31), which contains the peptide's basic residues, with the Ca-ATPase decreases the enzyme's V_{max} (Sasaki et al., 1992; Toyofuku et al., 1993), whereas the hydrophobic portion of the peptide (residues 28−47) decreases the Ca-ATPase's affinity for Ca^{2+} (Sasaki et al., 1992). Neutralization of PLB's basic charges via peptide phosphorylation relieves Ca-ATPase inhibition (Jones et al., 1985). Voss et al. (1994) have recently shown that the inhibitory influence of PLB on Ca-ATPase activity correlates strongly with PLB-induced aggregation of the enzyme (e.g., $f_1 = 0.5$ in cardiac SR), which is also relieved by neutralization of PLB's basic charges. The inhibitory influence of PLB on Ca-ATPase activity can be decreased significantly by increasing the ionic strength of the bulk solution but more efficiently by neutralizing basic charges at the SR membrane surface (Xu & Kirchberger, 1989; Chiesi & Schwaller, 1989). Finally, PLB inhibition of both Ca-ATPase activity and Ca-ATPase aggregation is severely diminished by micromolar Ca^{2+} (Voss et al., 1994). The plasma membrane Ca-pump is regulated by a basic, amphipathic autoinhibitory domain, homologous to PLB (Carafoli, 1992). The interaction of this domain with either calmodulin or acidic lipids relieves enzyme inhibition. A synthetic peptide corresponding to the plasma membrane autoregulatory domain has been added exogenously to the SR Ca-ATPase, resulting in Ca-dependent inhibition (Vorherr et al., 1992).

The number of recognized membrane surface-active peptides is growing (Raynor et al., 1991). We suggest that perturbations in the association state of target proteins due to peptide binding may be a common regulatory mechanism. For example, epidermal growth factor is known to affect its receptor by inducing self-association (Zidovetzki et al., 1986). Further spectroscopic studies should continue to provide

detailed information on which membrane components are targets for amphipathic peptides and the molecular mechanism of the peptide's action.

ACKNOWLEDGMENT

We thank Robert Bennett for constructing and maintaining the time-resolved phosphorescence spectrometer, and Franz Nisswandt and Nicoleta Cornea for computer programming. We are grateful to Brad Karon and Yongli Shi for their assistance with the FITC experiments. Razvan Cornea, Phuong Nguyen, and Erin Nissen provided excellent technical assistance in SR preparation and related assays.

REFERENCES

Alonso, G. L., & Hecht, J. P. (1990) *J. Theor. Biol. 147*, 161−176.
Asturias, F., & Blasie, J. K. (1991) *Biophys. J. 59*, 488−502.
Asturias, F. J., Fischetti, R. F., & Blasie, J. K. (1994) *Biophys. J. 66*, 1665−1677.
Bigelow, D. J., & Thomas, D. D. (1987) *J. Biol. Chem. 262*, 13449−13456.
Bigelow, D. J., Squier, T. C., & Thomas, D. D. (1986) *Biochemistry 25*, 194−202.
Bigelow, D. J., Squier, T. C., & Inesi, G. (1992) *J. Biol. Chem. 267*, 6952−6962.
Birmachu, W., & Thomas, D. D. (1990) *Biochemistry 29*, 3904−3914.
Birmachu, W., Voss, J. C., Louis, C. F., & Thomas, D. D. (1993) *Biochemistry 32*, 9445−9453.
Beeler, T., & Keffer, J. (1984) *Biochim. Biophys. Acta 773*, 99−105.
Campbell, K. P. (1986) in *Sarcoplasmic Reticulum in Muscle Physiology* (Entman, M. L., & Van Winkle, W. B., Eds.) Vol. I, pp 66−99, CRC Press, Inc., Boca Raton, FL.
Carafoli, E. (1992) *J. Biol. Chem. 267*, 2115−2118.
Chaloub, R. M., Guimaraes-Motta, H., Verjovski-Almeida, S., & de Meis, L. (1979) *J. Biol. Chem. 254*, 9464−9468.
Chen, P. S., Toribara, T. Y., & Warner, H. (1956) *Anal. Chem. 28*, 1756−1758.
Chiesi, M., & Schwaller, R. (1989) *FEBS Lett. 244*, 241−244.
Clarke, D. M., Loo, T. W., Inesi, G., & MacLennan, D. H. (1989) *Nature 339*, 476−478.
Coan, C., & Inesi, G. (1977) *J. Biol. Chem. 252*, 3044−3049.
Cuppoletti, J. (1990) *Arch. Biochem. Biophys. 283*, 409−415.
Cuppoletti, J., & Abbott, A. J. (1990) *Arch. Biochem. Biophys. 283*, 249−257.
Cuppoletti, J., Chernyak, B. V., Huang, P., & Malinowska, D. H. (1992) *Ann. N.Y. Acad. Sci. 671*, 443−445.
de Meis, L. (1988) *Methods Enzymol. 157*, 190−206.
Dempsey, C. E. (1990) *Biochim. Biophys. Acta 1031*, 143−161.
Dufton, M. J., Hider, R. C., & Cherry, R. J. (1984) *Eur. Biophys. J. 114*, 17−24.
Dupont, Y. (1980) *Eur. J. Biochem. 109*, 231−238.
Eads, T. M., Thomas, D. D., & Austin, R. H. (1984) *J. Mol. Biol. 179*, 55−81.
Ernst-Fonberg, M. L., Williams, S. G., & Worsham, L. M. S. (1990) *Biochim. Biophys. Acta 1046*, 111−119.
Fabiato, A. (1988) *Methods Enzymology 157*, 378−417.
Fernandez, J., Rosemblatt, M., & Hidalgo, C. (1980) *Biochim. Biophys. Acta 599*, 552−568.
Froehlich, J. P., & Taylor, E. W. (1975) *J. Biol. Chem. 250*, 2013−2021.
Froehlich, J. P., & Heller, P. F. (1985) *Biochemistry 24*, 126−136.
Froud, R. J., & Lee, A. (1986) *Biochem. J. 237*, 197−206.
Gornall, A., Bardawill, C., & David, M. (1949) *J. Biol. Chem. 177*, 751−766.
Gravitt, K. R., Ward, N. E., & O'Brian, C. A. (1994) *Biochem. Pharmacol. 47*, 425−427.
He, Z., Dunker, K., Wesson, C. R., & Trumble, W. R. (1993) *J. Biol. Chem. 268*, 24635−24641.
Henao, F., Orlowski, S., Merah, Z., & Champeil, P. (1992) *J. Biol. Chem. 267*, 10302−10312.
Hildago, C. (1987) *Crit. Rev. Biochem. 21*, 319−347.
Inesi, G. (1985) *Annu. Rev. Physiol. 47*, 573−601.
Itoh, N., & Kawakita, M. (1984) *J. Biochem. 95*, 661−669.
Jones L. R., Simmerman, H. K., Wilson, W. W., Gurd, F. R. N., & Wegener, A. D. (1985) *J. Biol. Chem. 260*, 7721−7730.
Karon, B. S., & Thomas, D. D. (1993) *Biochemistry 32*, 7503−7511.
Karon, B. S., Mahaney, J. E., & Thomas, D. D. (1994) *Biochemistry* (in press).
Kinosita, K., Jr., & Ikegami, A. (1984) *Biochem. Biophys. Res. Commun. 769*, 523−527.
Lewis, S. M., & Thomas D. D. (1986) *Biochemistry 25*, 4615−4621.
Lewis, S. M., & Thomas D. D. (1992) *Biochemistry 31*, 7381−7389.
Lipari, G., & Szabo, A. (1980) *Biophys. J. 30*, 489−506.
Ludescher, R. D., & Thomas, D. D. (1988) *Biochemistry 27*, 3343−3351.
Mahaney, J. E., & Thomas, D. D. (1991) *Biochemistry 30*, 7171−7180.
Mahaney, J. E., Kleinschmidt, J., Marsh, D., & Thomas, D. D. (1992) *Biophys. J. 63*, 1513−1522.
Mahaney, J. E., Froehlich, J. P., & Thomas, D. D. (1994) *Biophys. J. 66(2)*, A306.
Malencik, D. A., & Anderson, S. R. (1985) *Biochem. Biophys. Res. Commun. 130*, 22−29.
Martonosi, A. N., Jona, I., Molnar, E., Seidler, N., Buchet, R., & Varga, S. (1990) *FEBS Lett. 268*, 365−370.
Mersol, J. V., Kutchai, H., Mahaney, J. E., & Thomas, D. D. (1995) *Biochemistry* (in press).
Obara, M., Suzuki, H., & Kanazawa, T. (1988) *J. Biol. Chem. 263*, 3690−3697.
Paudel, H. K., Xu, Y.-H., Jarrett, H. W., & Carlson, G. M. (1993) *Biochemistry 32*, 11865−11872.
Petithory, J. R., & Jencks, W. P. (1986) *Biochemistry 25*, 4493−4497.
Raynor, R. L., Zheng, B., & Kuo, J. F. (1991) *J. Biol. Chem. 266*, 2753−2758.
Saffman, P. J., & Delbrück, M. (1975) *Proc. Natl. Acad. Sci. U.S.A. 72*, 3111−3113.
Sagara, Y., Wade, J. B., & Inesi, G. (1992a) *J. Biol. Chem 267*, 1286−1292.
Sagara, Y., Fernandez-Belda, F., de Meis, L., & Inesi, G. (1992b) *J. Biol. Chem 267*, 12606−12613.
Sasaki, T., Inui, M., Kimura, Y., Kuzuya, T., & Tada, M. (1992) *J. Biol. Chem. 267*, 1674−1679.
Segel, I. H. (1976) in *Biochemical Calculations,* second ed., Chapter 4, pp 208−323, John Wiley & Sons, New York.
Simmerman, H. K. B., Collins, J. H., Theibert, J. L, Wegener, A. D., & Jones, L. R. (1986) *J. Biol. Chem. 261*, 13333−13341.
Sprowl, C. D., & Thomas, D. D. (1989) *Biophys. J. 55*, 162a.
Squier, T. C., & Thomas, D. D. (1988) *J. Biol. Chem. 263*, 9171−9177.
Squier, T. C., Hughes, S. E., & Thomas, D. D. (1988a) *J. Biol. Chem. 263*, 9162−9170.

Squier, T. C., Bigelow, D. J., & Thomas, D. D. (1988b) *J. Biol. Chem. 263*, 9178−9186.

Teruel, J. A., & Inesi, G. (1988) *Biochemistry 27*, 5885−5890.

Thomas, D. D. (1986) in *Techniques for the Analysis of Membrane Proteins* (Ragan, C. I., & Cherry, R. J., Eds.) pp 377−431, Chapman & Hall, London.

Thomas, D. D., & Hidalgo, C. (1978) *Proc. Natl. Acad. Sci. U.S.A. 75*, 5488−5492.

Thomas, D. D., & Mahaney, J. E. (1993) *New Compr. Biochem. 25*, 301−320.

Thomas, D. D., & Karon, B. S. (1994) in *The Temperature Adaptation of Biological Membranes* (Cousins, A., Ed.) pp 1−12, Portland Press, London.

Toyofuku, T., Kurzydlowski, K., Tada, M., & MacLennan, D. H. (1993) *J. Biol. Chem. 268*, 2809−2815.

Vanderkooi, J. M., Ierokomas, A., Nakamura, H., & Martinosi, A. (1977) *Biochemistry 16*, 1262−1267.

Vorherr, T., Chiesi, M., Schwaller, R., & Carafoli, E. (1992) *Biochemistry 31*, 371−376.

Voss, J., Hussey, D., Birmachu, W., & Thomas, D. D. (1991) *Biochemistry 30*, 7498−7506.

Voss, J. C., Jones, L. R., & Thomas, D. D. (1994) *Biophys. J.* (in press).

Wakabayashi, S., Imagawa, T., & Shigekawa, M. (1990) *J. Biochem. (Tokyo) 107*, 563−571.

Werkmeister, J. A., Kirkpatrick, A., McKenzie, J. A., & Rivett, D. E. (1993) *Biochim. Biophys. Acta 1157*, 50−54.

Wictome, M., Henderson, I., Lee, A. G., & East, J. M. (1992) *Biochem. J. 283*, 525−529.

Wille, B. (1989) *Anal. Biochem. 178*, 118−120.

Xu, Z., & Kirchberger, M. A. (1989) *J. Biol. Chem. 264*, 16644−16651.

Zidovetzki, R., Yarden, Y., Schlessinger, J., & Jovin, T. M. (1986) *EMBO J. 5*, 247−250.

BI941362K